

# Chapter 2

## $^{134}\text{Cs}$ and $^{137}\text{Cs}$ in the Seawater Around Japan and in the North Pacific

Hideki Kaeriyama

**Abstract** Enormous quantities of radionuclides were released into the ocean via both atmospheric deposition and direct release as a result of the Fukushima Dai-ichi Nuclear Power Plant (FNPP) accident. The evaluation of FNPP-derived radioactive cesium (Cs) in the marine environment is important in addressing risks to both marine ecosystems and public health through consumption of fisheries products. Understanding the distribution patterns of radioactive Cs in the ocean throughout the water column is key in assessing its effects on marine ecosystems. This chapter summarizes the dispersion pattern of FNPP-derived radioactive Cs in the North Pacific and around Japan, based on our observational studies as follows: (1) eastward dispersion in surface seawater; (2) southwestward intrusion with mode water; and (3) background level  $^{137}\text{Cs}$  without any detectable  $^{134}\text{Cs}$  in the Japan Sea, East China Sea, Seto Inland Sea, and Bering Sea, along with highly radioactive Cs off the coast of East Japan.

**Keywords** Fukushima Dai-ichi Nuclear Power Plant accident •  $^{134}\text{Cs}$  •  $^{137}\text{Cs}$  • North Pacific • Kuroshio • Mode water

### 2.1 Fukushima Dai-ichi Nuclear Power Plant Accident

After the 9.0-magnitude Tohoku earthquake and the subsequent tsunami on March 11, 2011, loss of electric power at the Fukushima Dai-ichi Nuclear Power Plant (hereafter FNPP) resulted in overheated reactors and hydrogen explosions. Radioactive materials were then released into the ocean through atmospheric fallout as well as by direct release and leaking of the heavily contaminated coolant water (Chino et al. 2011; Buesseler et al. 2011). Because of its relatively long half-life (2.07 years for  $^{134}\text{Cs}$  and 30.07 years for  $^{137}\text{Cs}$ ), evaluation of this radioactive Cs in the marine environment is important for addressing risks to both marine ecosystems

---

H. Kaeriyama (✉)  
National Research Institute of Fisheries Sciences, Fisheries Research Agency,  
2-12-4, Fukuura, Kanazawa, Yokohama, Kanagawa 236-8648, Japan  
e-mail: [kaeriyama@affrc.go.jp](mailto:kaeriyama@affrc.go.jp)

and public health through consumption of fisheries products. The Japanese government conducted intensive monitoring of  $^{131}\text{I}$ ,  $^{134}\text{Cs}$ , and  $^{137}\text{Cs}$  in the seawater offshore near the FNPP (Nuclear Regulation Authority 2014) and in fisheries products from a wide area around Japan (Fisheries Agency 2014). Although information on radioactive contamination covering a broad area of the North Pacific is still quite limited (Aoyama et al. 2013a, b), some model experiments have addressed the dispersion of FNPP-derived radioactive Cs (Kawamura et al. 2011; Bailly du Bois et al. 2012; Dietze and Kriest 2012; Tsumune et al. 2012; Miyazawa et al. 2012), and estimated amounts of  $^{137}\text{Cs}$  discharged directly into the ocean ranged from 2.3 to 14.8 PBq, with considerable uncertainties (Masumoto et al. 2012). Although most studies have discussed the surface dispersion patterns of FNPP-derived radioactive Cs, understanding the ocean distribution patterns of radioactive Cs throughout the water column is key to assessing its effects on marine ecosystems.

## 2.2 Oceanic Background and $^{137}\text{Cs}$ in the North Pacific Before the FNPP Accident

The Kuroshio Current (KC) and its extension, Kuroshio Extension (KE), are the strongest eastward currents off the south and east coasts of Japan (Mizuno and White 1983). The KC and KE are important in the reproduction, dispersal, and migration of pelagic fish species (Sugisaki et al. 2010). Because the FNPP was located at  $37^{\circ}25.28'\text{N}$ ,  $141^{\circ}02.02'\text{E}$  (north of KE), most of the radioactive Cs released directly to the ocean was believed to be dispersed eastward in the North Pacific by the KE because the KE is thought to act as a transport barrier against southward dispersion (Buesseler et al. 2011, 2012; Aoyama et al. 2013a, b; Kaeriyama et al. 2013). In the northern area off the coast near the FNPP, the subarctic Oyashio water flows southwardly, and the water masses off the coast of East Japan, including off the FNPP, revealed complex features with meso-scale eddies as a result of the mixing of the subarctic Oyashio water and subtropical Kuroshio water (Yasuda 2003). The largest  $^{137}\text{Cs}$  deposition in the Pacific Ocean before the FNPP accident occurred in the early 1960s as a part of global fallout from atmospheric nuclear weapons testing (Povinec et al. 2004; Hirose and Aoyama 2003). In the North Pacific, the concentration of  $^{137}\text{Cs}$  in surface water ranged from 1.5 to  $2.0 \text{ Bq m}^{-3}$ , decay-corrected in 2011, and displayed a horizontally homogeneous distribution (Hirose and Aoyama 2003). Southward transport of  $^{137}\text{Cs}$  from the subarctic region (north of KE) to subtropical and tropical regions (south of KE) was observed at  $20^{\circ}\text{N}$ – $165^{\circ}\text{E}$  in 2002 (Aoyama et al. 2008). There were two  $^{137}\text{Cs}$  concentration maxima, located at the density range of North Pacific Subtropical Mode Water (NPSTMW) and Lighter Central Mode Water (Aoyama et al. 2008). The winter mixed layer south of the KE, which forms the NPSTMW core layer, develops and reaches its deepest depth from February to March, and the newly formed NPSTMW south of the KE is subducted and advected southwestward by the Kuroshio recirculation (Aoyama et al. 2008). The NPSTMW then begins to appear

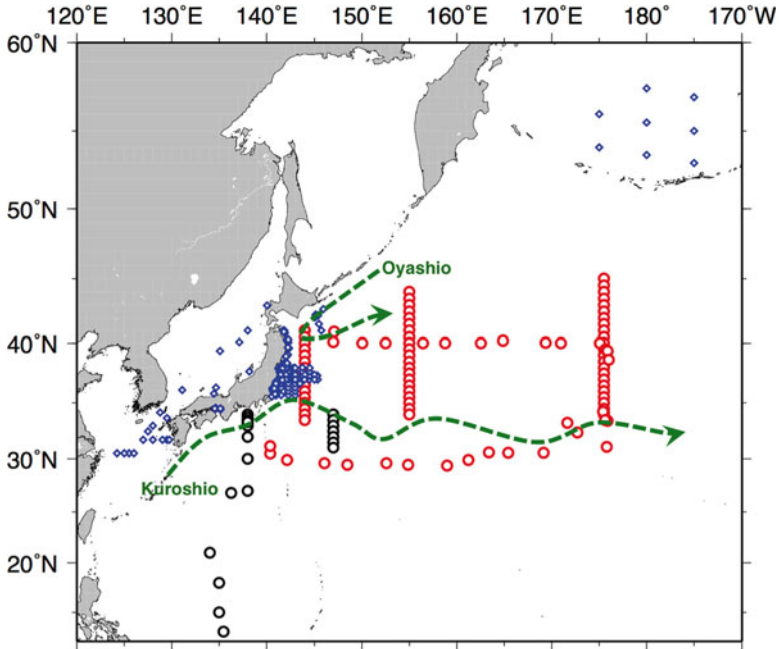


**Fig. 2.1** Sampling locations of seawater for measurement of  $^{134}\text{Cs}$  and  $^{137}\text{Cs}$  described in Sect. 2.3 (red open circles), in Sect. 2.4 (black open circles), and in Sect. 2.5 (blue open diamonds). Schematic flows of Kuroshio and Oyashio are indicated as green broken lines

at the southernmost Japanese islands within a few months (Oka et al. 2007). The  $^{137}\text{Cs}$  core waters observed at 20°N–165°E in 2002 were formed by the movement of mode waters between the 1960s and the 2000s (Aoyama et al. 2008).

This chapter consists of the following three descriptions concerning the distribution of  $^{134}\text{Cs}$  and  $^{137}\text{Cs}$  in seawater, based on our field observations after the FNPP accident (Fig. 2.1):

- Eastward dispersion of  $^{134}\text{Cs}$  and  $^{137}\text{Cs}$  in the western and central North Pacific (Kaeriyama et al. 2013, 2014c)
- Southwest intrusion of  $^{134}\text{Cs}$  and  $^{137}\text{Cs}$  with mode water (Kaeriyama et al. 2014a, c)
- $^{134}\text{Cs}$  and  $^{137}\text{Cs}$  around the Japanese Islands (Kaeriyama et al. 2014b, d)

### 2.3 Eastward Dispersion in Surface Seawater

During the summer season, 3-year repeated observations were conducted along three north–south transects at 144°E, 155°E, and 175°30'E in 2011 and 2013. In October 2011, additional sampling was conducted around the area covering summer season observations.

In July 2011, the concentrations of  $^{134}\text{Cs}$  and  $^{137}\text{Cs}$  in surface seawater were highly elevated, with values exceeding  $10\text{ Bq m}^{-3}$  and up to  $140\text{ Bq m}^{-3}$  and  $153\text{ Bq m}^{-3}$  at the northern end of the Kuroshio Extension (KE) along with  $144^\circ\text{E}$  and at all stations at  $155^\circ\text{E}$  (Fig. 2.2a). At  $38^\circ30'\text{N}$ – $144^\circ00'\text{E}$ ,  $^{134}\text{Cs}$  was not detected ( $<1.4\text{ Bq m}^{-3}$ ), and  $^{137}\text{Cs}$  concentration was lower than that detected at adjacent stations, despite being located at the north of the KE (Fig. 2.3). The concentrations of  $^{137}\text{Cs}$  in the central North Pacific ( $175^\circ30'\text{E}$  transect) ranged from  $3.2$  to  $9.3\text{ Bq m}^{-3}$  and were lower than those in the western part of the studied area ( $144^\circ\text{E}$  and  $155^\circ\text{E}$  transects) but still higher than background level ( $\sim 2.0\text{ Bq m}^{-3}$ ; Hirose and Aoyama 2003). In the northern section of the KE, an east–west gradient of  $^{134}\text{Cs}$  and  $^{137}\text{Cs}$  was observed in the surface water at the stations around  $40^\circ\text{N}$  in October 2011 (Fig. 2.2b). More than  $10\text{ Bq m}^{-3}$  of  $^{134}\text{Cs}$  and  $^{137}\text{Cs}$  was observed between  $147^\circ\text{E}$  and  $175^\circ05'\text{E}$ , and the highest concentrations were observed at  $152^\circ31'\text{E}$ . On the other hand, in the southern area of the KE, concentrations of  $^{137}\text{Cs}$  were relatively lower than those in the northern KE. A slight increase in  $^{137}\text{Cs}$  was observed at the eastern stations ( $31^\circ\text{N}$ – $34^\circ\text{N}$ , around  $175^\circ30'\text{E}$ ).  $^{134}\text{Cs}$  was not detected at almost any station located in the southern KE, mainly because of the short measurement time; the detection limit for  $^{134}\text{Cs}$  was  $3$ – $4\text{ Bq m}^{-3}$  with  $7,200\text{ s}$  counting. After 1 year from the observation in July 2011,  $^{134}\text{Cs}$  and  $^{137}\text{Cs}$  were drastically decreased at the  $144^\circ\text{E}$  and  $155^\circ\text{E}$  transects (Fig. 2.2c), and the concentrations of  $^{134}\text{Cs}$  and  $^{137}\text{Cs}$  at the  $175^\circ\text{E}$  transect between the 2 years were similar or slightly increased in July 2012 compared to July 2011. In July 2013, the concentrations of  $^{137}\text{Cs}$  were almost the same as background level at the  $144^\circ\text{E}$  and  $155^\circ\text{E}$  transects, and  $^{134}\text{Cs}$  was only detected at  $41^\circ30'\text{N}$ – $155^\circ\text{E}$  ( $1.9\text{ Bq m}^{-3}$ ). On the other hand,  $^{134}\text{Cs}$  was still detected at most stations ( $1.5$ – $5.8\text{ Bq m}^{-3}$ ), and the concentrations of  $^{137}\text{Cs}$  were slightly higher than those measured before the FNPP accident at the  $175^\circ30'\text{E}$  transect (Fig. 2.2d).

During the 3-year observations, FNPP-derived Cs was high in the northern KE and low in the southern KE. The low concentration of radioactive Cs in the southern KE was also confirmed by field observations of seawater (Buesseler et al. 2011, 2012; Aoyama et al. 2012) and simulation models (Masumoto et al. 2012). Thus, the majority of radioactive Cs directly released to the ocean from the FNPP was not dispersed south of the KE near the east coast of Japan in 2011; rather, the detection of  $^{134}\text{Cs}$  at three stations along with the  $175^\circ30'\text{E}$  transect and station located south of the KE ( $35^\circ\text{N}$ – $144^\circ\text{E}$ ) in July 2011 and stations around  $30^\circ\text{N}$  in October 2011 may indicate the effect of atmospheric deposition. Atmospheric deposition occurred mostly in March 2011 (Chino et al. 2011), and most of the direct discharge occurred during late March and early April 2011 (Tsumune et al. 2012). Aoyama et al. (2013b) reported a high radioactive Cs concentration area around the International Date Line in April–July 2011. The eastward speed of the radioactive plume was estimated to be  $8\text{ cm s}^{-1}$ . Moreover, atmospheric deposition of radioactive Cs and  $^{131}\text{I}$  south of the KE near the east coast of Japan was strongly indicated by numerical simulations (Kawamura et al. 2011; Kobayashi et al. 2013). Thus, the highly radioactive Cs area observed in the central North Pacific in July 2011 and south of the KE near the east coast of Japan may have originated from atmospheric deposition.

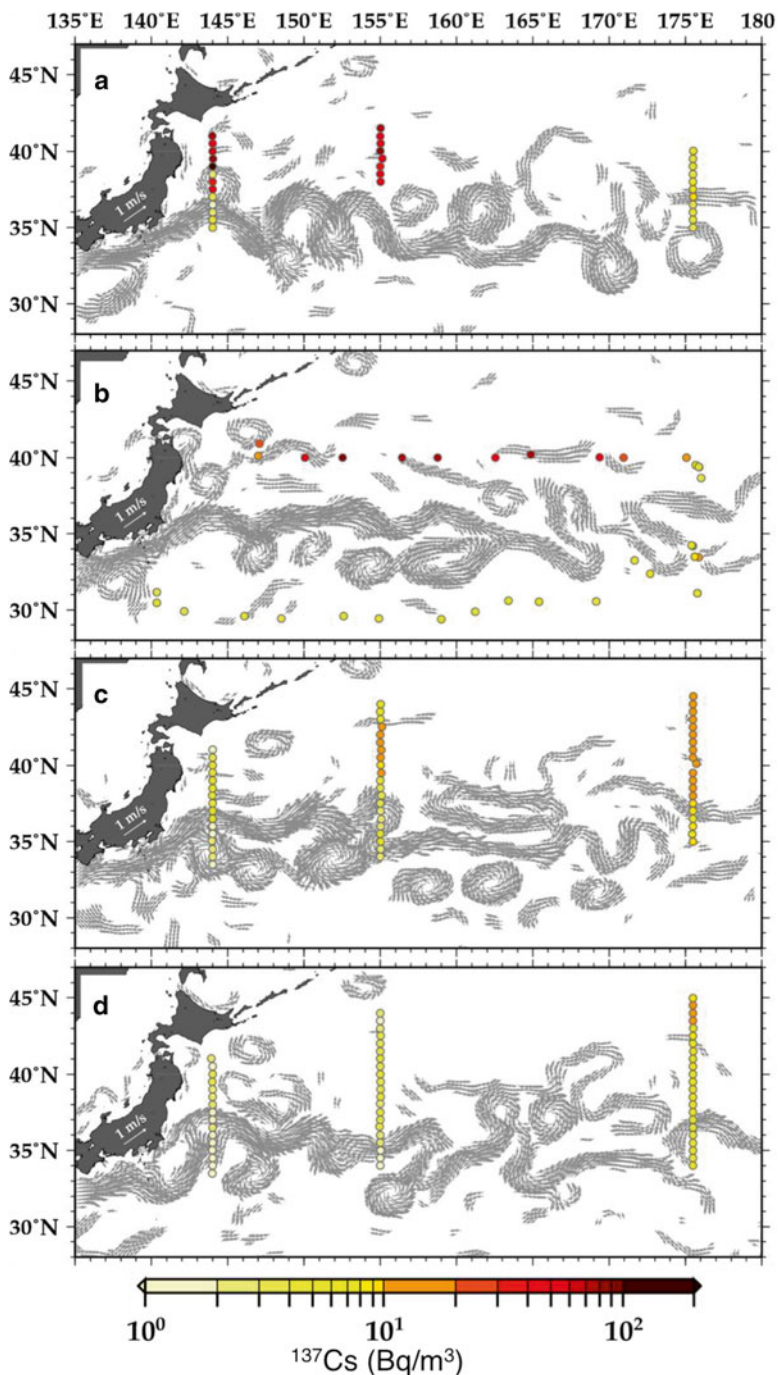


**Fig. 2.2** Sampling locations for surface seawater in the western and central North Pacific. *Closed circles* indicate the sampling stations. *Color of the closed circles* indicates the concentration of  $^{137}\text{Cs}$  in the surface seawater. *Gray arrows* indicate the estimated temporal mean velocity vectors for the period between June 30 and July 29, 2011 (a), October 14 and November 7, 2011 (b), July 2 and August 1, 2012 (c), and July 2–31, 2013 (d). (Modified from Kaeriyama et al. 2013)

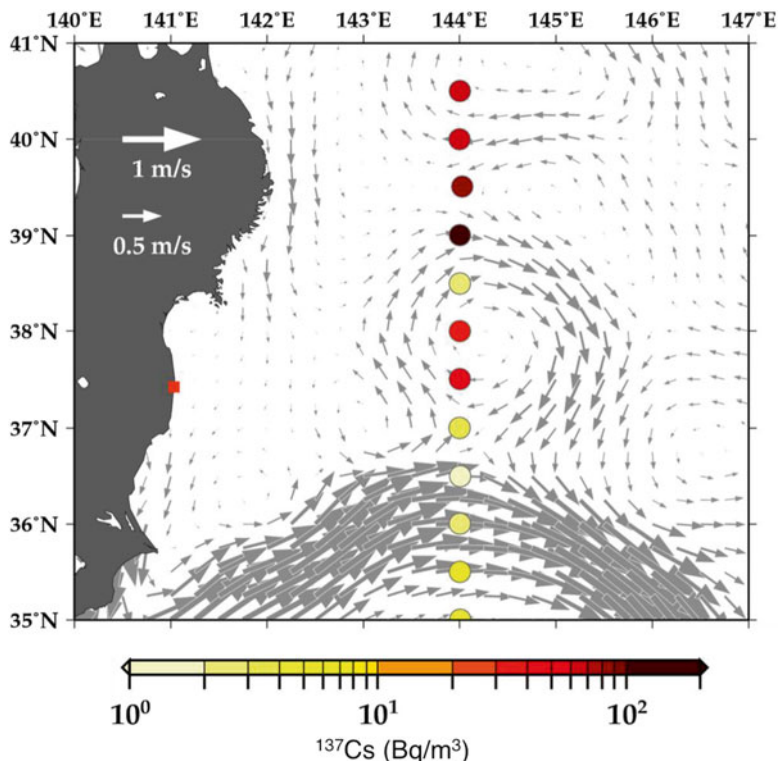


**Fig. 2.3** Sampling locations for surface seawater around the anti-cyclonic eddy observed in July 2011. Color of the closed circles indicates concentration of  $^{137}\text{Cs}$  in the surface seawater. Gray arrows indicate the estimated temporal mean velocity vectors for the period between June 30 and July 29, 2011 (Modified from Kaeriyama et al. 2013)

Some patchy distribution of radioactive Cs was also observed; local minima of  $^{137}\text{Cs}$  and  $^{134}\text{Cs}$  were observed at  $38^{\circ}30'\text{N}$ – $144^{\circ}\text{E}$ , whereas the adjacent stations had higher concentrations in July 2011 (Fig. 2.3). Judging from the sea surface velocity field,  $38^{\circ}30'\text{N}$ – $144^{\circ}\text{E}$  was located at the edge of an anti-cyclonic eddy (Fig. 2.3). Because the surface water of anti-cyclonic eddies originates from the KE (Itoh and Yasuda 2010a; Yasuda et al. 1992), the water at  $38^{\circ}30'\text{N}$ – $144^{\circ}\text{E}$  would not contain much water derived from the FNPP. As there are many meso-scale eddies that originate from both the KE and Oyashio in the western Kuroshio–Oyashio transition area (Itoh and Yasuda 2010b), the concentration of radioactive Cs should be patchy corresponding to eddies there. An area with high concentration (more than  $50 \text{ Bq m}^{-3}$ ) of  $^{137}\text{Cs}$  was distributed around  $40^{\circ}\text{N}$  between  $150^{\circ}\text{E}$  and  $170^{\circ}\text{E}$  in October 2011 (Fig. 2.2b). As Isoguchi et al. (2006) showed the existence of two quasi-stationary jets that flow northeastward from the KE to the subarctic front between  $150^{\circ}\text{E}$  and  $170^{\circ}\text{E}$ , radioactive Cs from the FNPP might have dispersed along these jets around the time of this observation period.



The concentrations of radioactive Cs at the  $144^\circ\text{E}$  and  $155^\circ\text{E}$  transects in July 2012 were much less than those in the previous year (July 2011). These differences strongly suggest that the water with a high concentration of radioactive Cs had been transported eastward by 16 months after the FNPP accident. In contrast, the concentrations of radioactive Cs at the  $175^\circ30'\text{E}$  transect were similar between the 2 years. The concentration of radioactive Cs observed at the  $175^\circ30'\text{E}$  transect in July 2012 would have been a result of dilution processes that occurred in the western North Pacific during the 16 months since the FNPP accident. Because the KE jet weakens eastward and its streamline spreads northward or southward by  $175^\circ\text{E}$  (see fig. 1 of Qiu and Chen 2011), the highly radioactive Cs waters would be stagnant around the central Pacific and would disperse not only eastward but also slowly northward and southward. Actually,  $^{134}\text{Cs}$  was still detected at the  $175^\circ30'\text{E}$  transect, but it was not detected at the  $144^\circ\text{E}$  and  $155^\circ\text{E}$  transects, except for that at  $41^\circ30'\text{N}$ ,  $155^\circ\text{E}$  in 2013.

A considerable amount of radioactive Cs from the FNPP was dispersed eastward from the western North Pacific to the central North Pacific during the first year after the FNPP accident. In addition, it dispersed not only eastward but also northward and southward in the central North Pacific for 2 to 3 years after the FNPP accident (Kaeriyama et al. 2013).

## 2.4 Southwest Intrusion with Mode Water

A repeat observation was conducted four to five times per year between  $27^\circ\text{N}$  and  $34^\circ\text{N}$  along  $138^\circ\text{E}$  during August 2011 and March 2013. As the  $138^\circ\text{E}$  transect lies across the Kuroshio Current (KC), the water samples were collected north of the KC, in the KC, and south of the KC. In September 2012, additional sampling was conducted at five stations located far south of Japan between  $13^\circ\text{N}$  and  $26^\circ50'\text{N}$  around  $135^\circ\text{E}$ . In October 2011 and November 2012, seawater samples were also collected between  $30^\circ30'\text{N}$  and  $36^\circ30'\text{N}$  along  $147^\circ\text{E}$  near the Kuroshio Extension (KE) (Fig. 2.1).

### 2.4.1 *Transect Across the Kuroshio Current*

For the nine observations along the  $138^\circ\text{E}$  transect, the concentration of  $^{137}\text{Cs}$  at all sampling depths ranged from 1.3 to 3.7  $\text{Bq m}^{-3}$  at  $34^\circ\text{N}$  (north of the KC), and from 1.2 to 2.6  $\text{Bq m}^{-3}$  in the KC. No  $^{134}\text{Cs}$  was detected except at 100 m in the KC in January 2012. The vertical distribution pattern of  $^{137}\text{Cs}$  at the stations north of and in the KC was relatively uniform throughout the water column between 0 and 500 m, whereas  $^{137}\text{Cs}$  concentrations south of the KC had significant peaks (2.3–12  $\text{Bq m}^{-3}$ ) at subsurface depths (100–500 m), especially after April 2012 (Fig. 2.4). We also detected  $^{134}\text{Cs}$  at the subsurface peak of  $^{137}\text{Cs}$  (mostly at 300 m), which

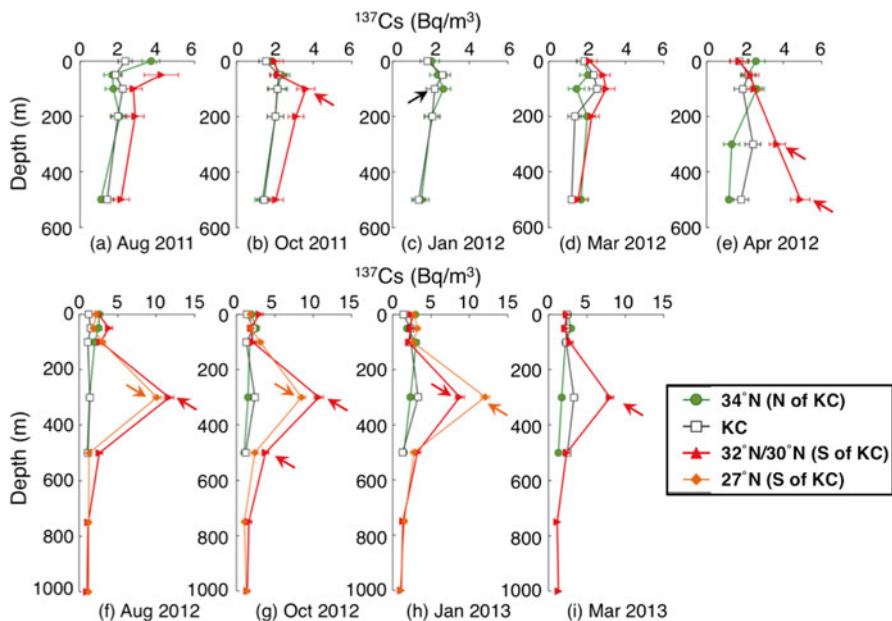


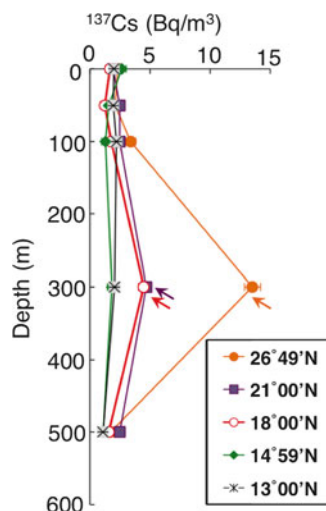
**Fig. 2.4** Vertical profiles of  $^{137}\text{Cs}$  at three to four stations along the  $138^\circ\text{E}$  line during August 2011 and March 2013. *Arrows* indicate the detection of  $^{134}\text{Cs}$ . *Error bars* indicate counting error ( $\pm 1\sigma$ ). When  $^{137}\text{Cs}$  was under the detection limit ( $<3\sigma$ ), the detection limit was plotted (Adopted with permission from Kaeriyama et al. 2014a. Copyright (2014) American Chemical Society)

varied from  $1.8$  to  $6.8 \text{ Bq m}^{-3}$  south of the KC. The concentration of  $^{137}\text{Cs}$  in deeper water ( $\geq 750 \text{ m}$ ) was lower than  $1.6 \text{ Bq m}^{-3}$ , and no  $^{134}\text{Cs}$  was detected. Thus, the subsurface peak of  $^{134}\text{Cs}$  and  $^{137}\text{Cs}$  was observed between  $100$  and  $500 \text{ m}$  south of the KC. Further south of the  $138^\circ\text{E}$  transect,  $^{134}\text{Cs}$  was also detected at  $300 \text{ m}$ , and  $^{137}\text{Cs}$  ranged from  $1.2$  to  $14 \text{ Bq m}^{-3}$  between  $0$  and  $500 \text{ m}$  in September 2012 between  $18^\circ\text{N}$  and  $26^\circ 49'\text{N}$  around  $135^\circ\text{E}$ . The  $^{137}\text{Cs}$  concentration was relatively low and vertically homogenized, and  $^{134}\text{Cs}$  was not detectable at  $14^\circ 59'\text{N}$  or  $13^\circ\text{N}$  on the same cruise (Fig. 2.5). The  $^{137}\text{Cs}$  inventories were nearly the same level, between  $630 \pm 180$  and  $1,160 \pm 190 \text{ Bq m}^{-2}$ , both north of the KC and in the KC during the entire study period (Fig. 2.6a). South of the KC, the inventories were comparable with those found north of the KC and in the KC during August 2011 and February 2012 ( $1,000$ – $1,350 \text{ Bq m}^{-2}$ ) and then markedly increased to  $3,260 \pm 410 \text{ Bq m}^{-2}$  after April 2012 (Fig. 2.6a). The inventories of  $^{137}\text{Cs}$  ranged from  $800 \pm 300$  to  $3,460 \pm 560 \text{ Bq m}^{-2}$  and decreased traveling southward between  $13^\circ 00'\text{N}$  and  $26^\circ 49'\text{N}$  around  $135^\circ\text{E}$  in September 2012 (Fig. 2.6b).

Because water usually circulates along the isopycnal layer below the subsurface, the density range of the subsurface peak of  $^{134}\text{Cs}$  and  $^{137}\text{Cs}$  gives information about what water mass transported FNPP-derived radioactive Cs. Although the subsurface peaks were found at the isopycnals from  $25.0$  to  $25.5 \sigma_\theta$  and from  $26.0$  to  $26.5 \sigma_\theta$  at  $34^\circ 46'\text{N}$ ,  $148^\circ 52'\text{E}$  in February 2012 (Kumamoto et al. 2013), the present study



**Fig. 2.5** Vertical profiles of  $^{137}\text{Cs}$  at five stations around  $135^\circ\text{E}$  in September 2012. *Arrows indicate the detection of  $^{134}\text{Cs}$ . Error bars indicate counting error ( $\pm 1\sigma$ ). When  $^{137}\text{Cs}$  was below the detection limit ( $<3\sigma$ ), the detection limit was plotted (Adopted with permission from Kaeriyama et al. 2014a. Copyright (2014) American Chemical Society)*



shows that  $^{134}\text{Cs}$  south of the KC along  $138^\circ\text{E}$  and around  $135^\circ\text{E}$  was observed at a density range from  $23.9$  to  $25.7 \sigma_\theta$ , with a sharp peak around  $25.3 \sigma_\theta$  (Fig. 2.7). The  $^{134}\text{Cs}$  peak at  $25.3 \sigma_\theta$  suggests that core waters with high  $^{134}\text{Cs}$  and  $^{137}\text{Cs}$  levels derived from the FNPP accident are distributed in the North Pacific Subtropical Mode Water (NPSTMW). The predominant temperature ( $16.4$ – $17.9$  °C) and salinity ( $34.6$ – $34.7$  psu) ranges of  $^{134}\text{Cs}$  and  $^{137}\text{Cs}$  are present within the NPSTMW (Oka 2009). In the present study, the radioactive Cs detected in the southern region was thought to contain the atmospheric fallout from the FNPP to the sea surface south of the KE during mid-March and early April 2011 (Sect. 2.3; Chino et al. 2011; Rypina et al. 2013; Honda et al. 2012; Kobayashi et al. 2013).

Using dissolved oxygen data (apparent oxygen utilization, AOU) (Ebbesmeyer and Lindstrom 1986), we examined whether the subsurface water was ventilated with highly radioactive Cs at the surface in March 2011 as oxygen in the NPSTMW gradually decreases after its subduction (Suga and Hanawa 1995). The detected  $^{134}\text{Cs}$  south of the KC in April 2012 and in January 2013 did in fact originate from atmospheric deposition and was ventilated in March 2011 (Kaeriyama et al. 2014a). The inventory of  $^{137}\text{Cs}$  south of the KC along the  $138^\circ\text{E}$  transect increased from  $1,100$  to  $3,210 \text{ Bq m}^{-2}$  between February and August 2012 (Fig. 2.6a), suggesting that the newly formed NPSTMW brought more FNPP-derived radioactive Cs to the south of the KC. Alternatively, the inventories of  $^{137}\text{Cs}$  north of the KC and in the KC along the  $138^\circ\text{E}$  transect varied from  $650$  to  $1,410 \text{ Bq m}^{-2}$  throughout the study period (Fig. 2.6a), which is almost comparable with the water column inventories of  $^{137}\text{Cs}$  detected in the North Pacific before the FNPP accident (almost  $1,000 \text{ Bq m}^{-2}$ ) Aoyama et al. 2008; Povinec et al. 2004). These data may indicate that the water north of and in the KC was mostly unaffected by the FNPP-derived radioactive Cs. In September 2012,  $^{134}\text{Cs}$  was detected at  $18^\circ\text{N}$ , but not at  $14^\circ59'\text{N}$  (Fig. 2.5). The inventories of  $^{137}\text{Cs}$  at  $13^\circ\text{N}$  and  $14^\circ59'\text{N}$  (Fig. 2.6b) were comparable with those in

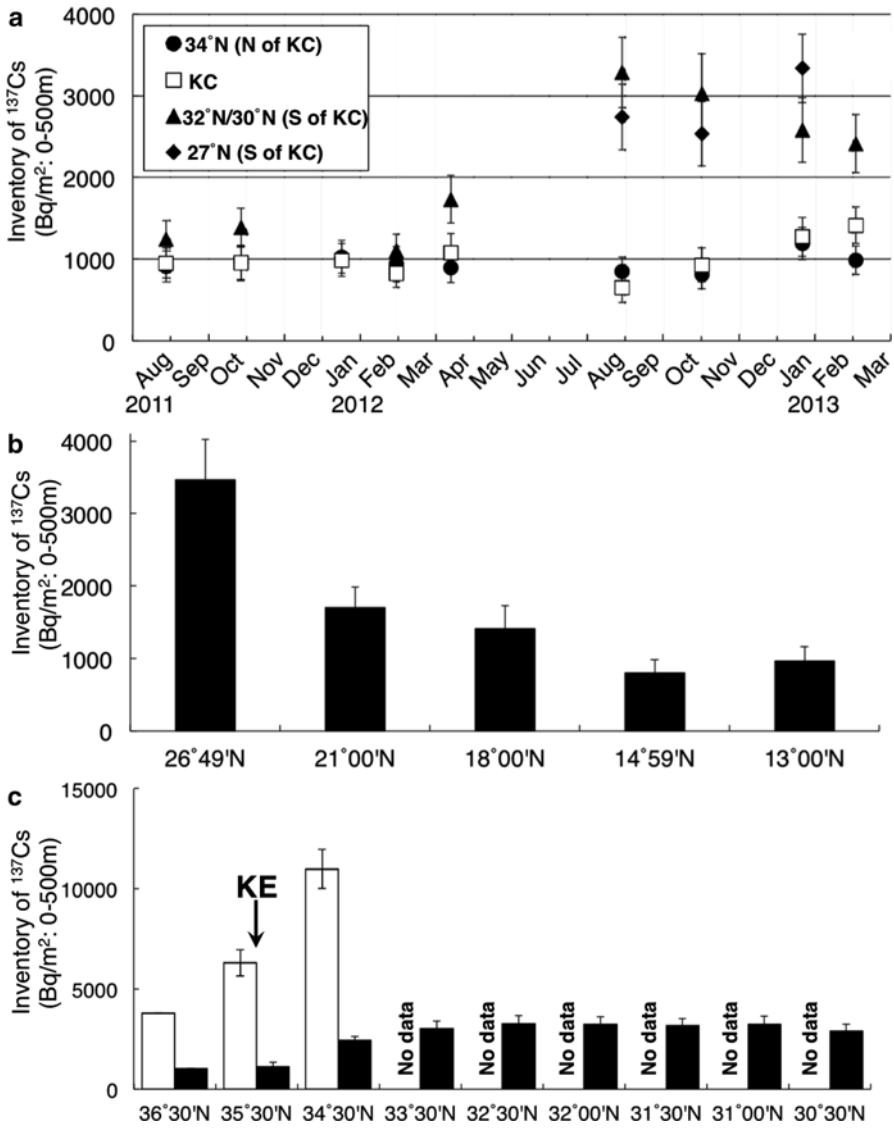
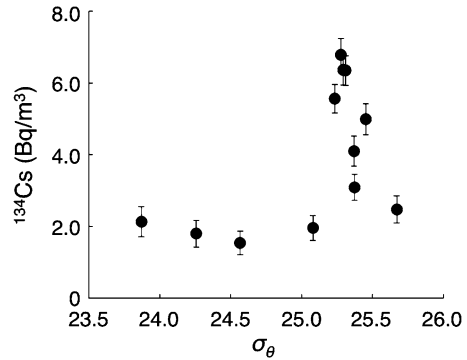


**Fig. 2.6** Water column inventories of <sup>137</sup>Cs between 0- and 500-m depth along the 138°E transect from August 2011 to March 2013 (a), around 135°E in September 2012 (b), and along 147°E in October 2011 (*open bars*) and November 2012 (*closed bars*) (c). When <sup>137</sup>Cs was under the detection limit (<3σ), the detection limit was used for calculation (Adopted with permission from Kaeriyama et al. 2014a. Copyright (2014) American Chemical Society)

**Fig. 2.7** Relationship between subsurface ( $\geq 100$  m depth)  $^{134}\text{Cs}$  concentration and potential density ( $\sigma_\theta$ ) south of the Kuroshio Current (KC) along the  $138^\circ\text{E}$  transect (Adopted with permission from Kaeriyama et al. 2014a. Copyright (2014) American Chemical Society)



the North Pacific before the FNPP accident (Aoyama et al. 2008; Povinec et al. 2004). These results suggest the FNPP-derived radioactive Cs core water had dispersed southward to at least  $18^\circ\text{N}$  by 19 months after the FNPP accident. Nakano and Povinec (2012) reported long-term simulations of FNPP-derived  $^{137}\text{Cs}$  dispersion in the global oceans with a grid size of  $2 \times 2$  and 15 layers of vertical direction. The vertical distribution pattern of FNPP-derived  $^{137}\text{Cs}$  with subsurface peaks between 100 and 300 m at  $20^\circ\text{N}$ – $130^\circ\text{E}$  is in agreement with our results at  $21^\circ\text{N}$ – $134^\circ\text{E}$  from September 2012 (Fig. 2.5). However, the timing of the appearances and concentrations of subsurface  $^{137}\text{Cs}$  peaks are very different from our results. Their model results revealed the first appearance of a subsurface peak of FNPP-derived  $^{137}\text{Cs}$  was in 2014 and the peak depth concentration was estimated as  $0.5 \text{ Bq m}^{-3}$ . However, our results showed a subsurface peak concentration of  $2.1 \text{ Bq m}^{-3}$  for FNPP-derived  $^{134}\text{Cs}$  at  $20^\circ\text{N}$ – $130^\circ\text{E}$  in September 2012, that is, 2 years earlier than the model result. These differences between the modeled result of Nakano and Povinec (2012) and our direct observation may be the result of limitations such as uncertainties regarding the amount of  $^{137}\text{Cs}$  released from the FNPP and the resolution of the velocity field. Nakano and Povinec (2012) mentioned that the KC and the KE were weaker in their model than the ARGO drifters predicted.

#### 2.4.2 *Transect Across the Kuroshio Extension*

In October 2011, concentrations of  $^{134}\text{Cs}$  and  $^{137}\text{Cs}$  in excess of  $20 \text{ Bq m}^{-3}$  were observed in surface waters and at 50-m depth north of the KE at  $147^\circ\text{E}$  (Fig. 2.8). Alternatively, the subsurface peak of radioactive Cs was observed in the KE and south of the KE (Fig. 2.8). The concentrations of  $^{137}\text{Cs}$  drastically decreased after 1 year at all three stations and were distributed uniformly between  $1.3$  and  $4.3 \text{ Bq m}^{-3}$ , which were observed north of and in the KE in November 2012 (Fig. 2.8). In contrast, the subsurface peak of  $^{137}\text{Cs}$  was observed at  $9$  to  $12 \text{ Bq m}^{-3}$  south of the KE, with  $^{134}\text{Cs}$  detected in the KE and south of the KE in November 2012 (Fig. 2.8). Southeast of the FNPP,  $^{137}\text{Cs}$  inventories north of the KE, in the KE, and south of the KE in October 2011 were calculated to be  $3,840 \pm 660$ ,  $6,370 \pm 2,060$ , and  $10,990 \pm 3,870 \text{ Bq m}^{-2}$ ,

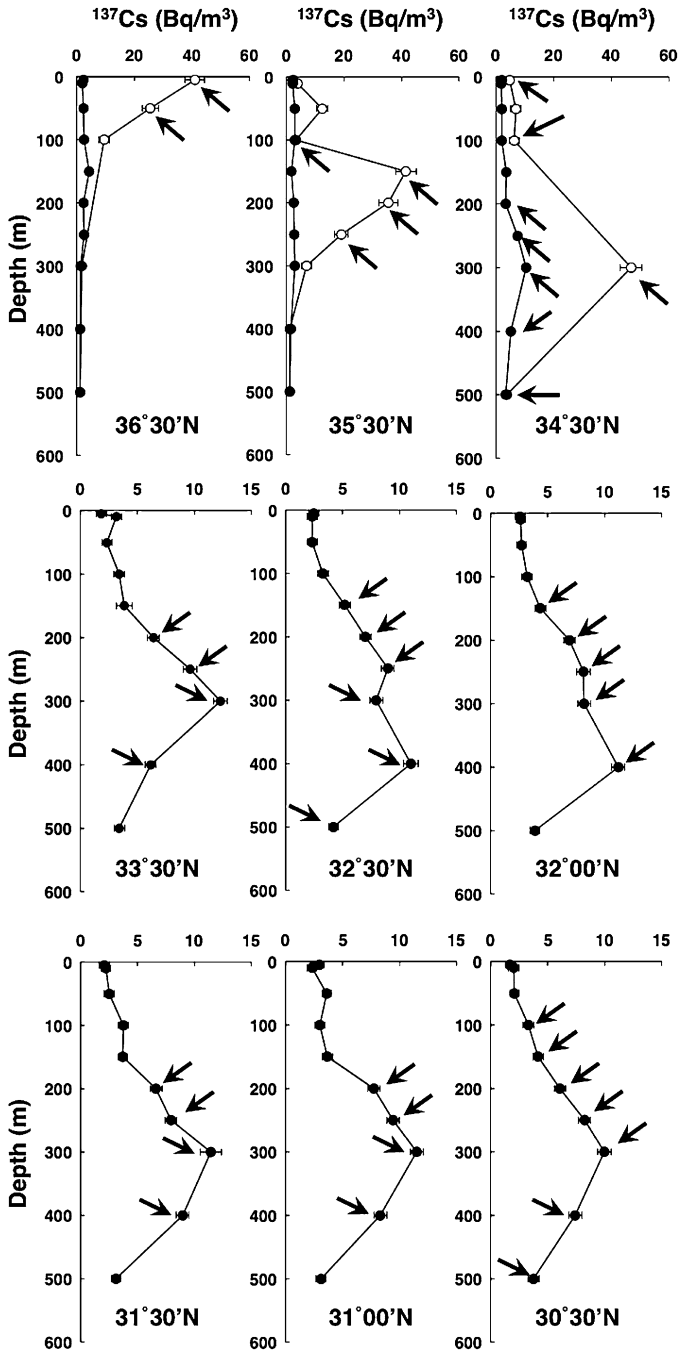


**Fig. 2.8** Vertical profiles of  $^{137}\text{Cs}$  north of the Kuroshio Extension (KE) ( $36^{\circ}30'N$ ), in the KE ( $35^{\circ}30'N$ ), and south of KE ( $30^{\circ}00'N$ - $34^{\circ}30'N$ ). *Open circles* represent values recorded in October 2011. *Closed circles* represent values recorded in November 2012. *Arrows* indicate the detection of  $^{134}\text{Cs}$ . *Error bars* indicate counting error ( $\pm 1\sigma$ ). When  $^{137}\text{Cs}$  was under the detection limit ( $<3\sigma$ ), the detection limit was plotted

respectively (Fig. 2.6c); those from November 2012 were  $1,030 \pm 280$ ,  $1,150 \pm 370$ , and between 2,440 and 3,300 Bq  $\text{m}^{-2}$ , respectively (Fig. 2.6c).

In shallow water (0 and 50-m depth), high concentrations of  $^{134}\text{Cs}$  and  $^{137}\text{Cs}$  were observed north of the KE, but low concentrations were observed in the KE and south of the KE, which is consistent with previous studies showing that the KE prevented the southward dispersion of radioactive Cs from the FNPP in the surface water (Sect. 2.3; Aoyama et al. 2013a, b; Buesseler et al. 2012). Our results showed that deeper intrusion of FNPP-derived radioactive Cs occurred at  $34^\circ 30' \text{N}$  and  $35^\circ 30' \text{N}$  in October 2011 before the first winter after the FNPP accident. In October 2011, the subsurface peak of  $^{134}\text{Cs}$  was observed from 24.0 to 26.5  $\sigma_\theta$ . Observations at  $34^\circ 30' \text{N}$  in November 2012 were between 25.1 and 26.1  $\sigma_\theta$  with a peak at 25.3  $\sigma_\theta$ . The difference in the density of subsurface  $^{134}\text{Cs}$  waters may indicate that different water masses of FNPP-derived radioactive Cs existed during these 2 years. The large spatial variation of the FNPP-derived radioactive Cs around the KE was also discussed with data obtained at  $34^\circ 46' \text{N}$ – $148^\circ 52' \text{E}$  in February 2012 (Kumamoto et al. 2013). Rypina et al. (2013) reported model results of FNPP-derived radioactive Cs in the area of  $34^\circ \text{N}$ – $37^\circ \text{N}$ ,  $142^\circ \text{E}$ – $147^\circ \text{E}$  during March and June 2011. The three-dimensional (3-D) model results (fig. 9 of Rypina et al. 2013) suggested that FNPP-derived  $^{137}\text{Cs}$  occasionally penetrated to 300–400 m in depth north of the KE during April and June 2011 as a consequence of the spatial heterogeneity of mixed-layer depth and the existence of strong downwelling regions. Furthermore, Oikawa et al. (2013) showed data obtained near the FNPP during March 2011 and February 2012, which were part of the monitoring program initiated by the Ministry of Education, Culture, Sports, Science and Technology (MEXT). They concluded that the depth of  $\sigma_t$  isopycnals of 25.5–26.5 waters increased with time and transported the FNPP-derived radioactive Cs to deep water from the FNPP-proximal coastal waters between May and December 2011. Taking into account the monitoring data of MEXT (Oikawa et al. 2013), the observational data from February 2012 (Kumamoto et al. 2013), and model results (Rypina et al. 2013), it has been suggested that the subsurface peak of radioactive Cs observed south of and in the KE in October 2011 may have been transported from the coastal area off the FNPP without subduction.

### 2.4.3 Amount of $^{134}\text{Cs}$ in Subsurface Core Waters in the Southern Area

We estimated the amount of  $^{134}\text{Cs}$  in subsurface core waters south of both the KC and the KE from our observational data collected in September 2012, when the southernmost detection of  $^{134}\text{Cs}$  was observed at  $18^\circ \text{N}$ – $135^\circ \text{E}$  (Fig. 2.5). Results suggest that the FNPP-derived radioactive Cs was taken into the NPSTMW and then transported southwestward by the Kuroshio recirculation (Suga and Hanawa 1995). As a first step, the amount of  $^{134}\text{Cs}$  in the entire area of the NPSTMW was estimated. The average concentration of  $^{134}\text{Cs}$  in the NPSTMW ( $26^\circ 49' \text{N}$ – $34^\circ 30' \text{N}$ ), decay-corrected on March 11, 2011, was  $11 \pm 1.7$  Bq  $\text{m}^{-3}$ . Suga et al. (2008) estimated the total volume of the NPSTMW as  $1 \times 10^6$   $\text{km}^3$ . Therefore, the amount of

$^{134}\text{Cs}$  in the entire area of the NPSTMW would be estimated as  $11 \pm 1.7$  PBq. Kumamoto et al. (2014) reported  $^{134}\text{Cs}$  in the area around the center of the NPSTMW during January and February 2012, estimating the total inventory of  $^{134}\text{Cs}$  in the NPSTMW to be 6 PBq. These estimates may indicate that 6 PBq of  $^{134}\text{Cs}$  intruded into the NPSTMW during March and April 2011, as observed in January and February 2012 (Kumamoto et al. 2014), and 3.3–6.7 PBq additional  $^{134}\text{Cs}$  had intruded into the NPSTMW during the 2011–2012 winter season, observed in September 2012 (this study). Because the vertical resolution of this study was low (seven layers between the surface and 1,000 m), and the study area was limited to the western part of the NPSTMW, considerable uncertainty should have been taken into account. The second estimate was limited to the peak depth of radioactive Cs around the western part of the NPSTMW. Contours of acceleration potential on an isopycnal surface indicate isopycnal streamlining in September 2012 based on ARGO float data. The shape of the closed contour line of  $19 \text{ m}^2 \text{ s}^{-2}$  is similar to the Kuroshio recirculation as described by Suga and Hanawa (1995), and the area was defined as the western part of the NPSTMW (Fig. 2.9a).

The  $^{134}\text{Cs}$  concentration was estimated for the observationally sparse area in the western part of the NPSTMW by Gaussian averaging (Fig. 2.9b). The thickness of the NPSTMW core was estimated as the difference between the depths of isopycnal surfaces  $25.2 \sigma_\theta$  and  $25.4 \sigma_\theta$  (Fig. 2.9c). The horizontal inventory of  $^{134}\text{Cs}$  in the western part of the NPSTMW core was estimated using the product of the concentration and thickness listed above (Fig. 2.9d). Then, the amount of  $^{134}\text{Cs}$  in the core of the western part of the NPSTMW in September 2012 was estimated to be 1.07 PBq, which accounts for 7–47 % of the total amount of  $^{134}\text{Cs}$  released directly into the ocean from the FNPP (2.3–14.8 PBq of  $^{137}\text{Cs}$ ;  $^{134}\text{Cs}/^{137}\text{Cs}$  ratio assumed to be 1.0 Masumoto et al. 2012), or 10 % of the total deposition including direct release and atmospheric surface deposition (11 PBq  $^{134}\text{Cs}$ ; Kobayashi et al. 2013). Although the estimation includes enormous uncertainties, it should be noted that a considerable amount of the FNPP-derived radioactive Cs had been dispersed in the southwestern portion of the North Pacific across the KC, which was considered to act as a barrier against the southward dispersion of FNPP-derived radionuclides (Sect. 2.3, Aoyama et al. 2013a, b; Buesseler et al. 2012). To clarify and improve the amount of FNPP-derived radioactive Cs in the southwestern portion of the North Pacific, future studies should include not only collection of observational data, but also an improved model with a comprehensive understanding of FNPP-derived Cs dispersion in the oceanic environment.

---

**Fig. 2.9** (continued) **(b)** Estimated spatial distribution of  $^{134}\text{Cs}$  concentration ( $\text{Bq m}^{-3}$ ) at the core water of the western part of the NPSTMW, which is estimated by Gaussian averaging with a 1,000-km e-folding scale applied to the  $^{134}\text{Cs}$  data collected during September and November 2012 and decay-corrected on March 11, 2011. The *black line* indicates acceleration potential of  $19 \text{ m}^2 \text{ s}^{-2}$ . **(c)** Spatial distribution of water thickness between the isopycnal surfaces  $25.2 \sigma_\theta$  and  $25.4 \sigma_\theta$  based on the Argo data. **(d)** Estimated inventory of  $^{134}\text{Cs}$  in the core water of the western part of the NPSTMW in September 2012, which is estimated by the  $^{134}\text{Cs}$  concentration ( $\text{Bq m}^{-3}$ ) and the water column thickness. The *black line* indicates acceleration potential of  $19 \text{ m}^2 \text{ s}^{-2}$



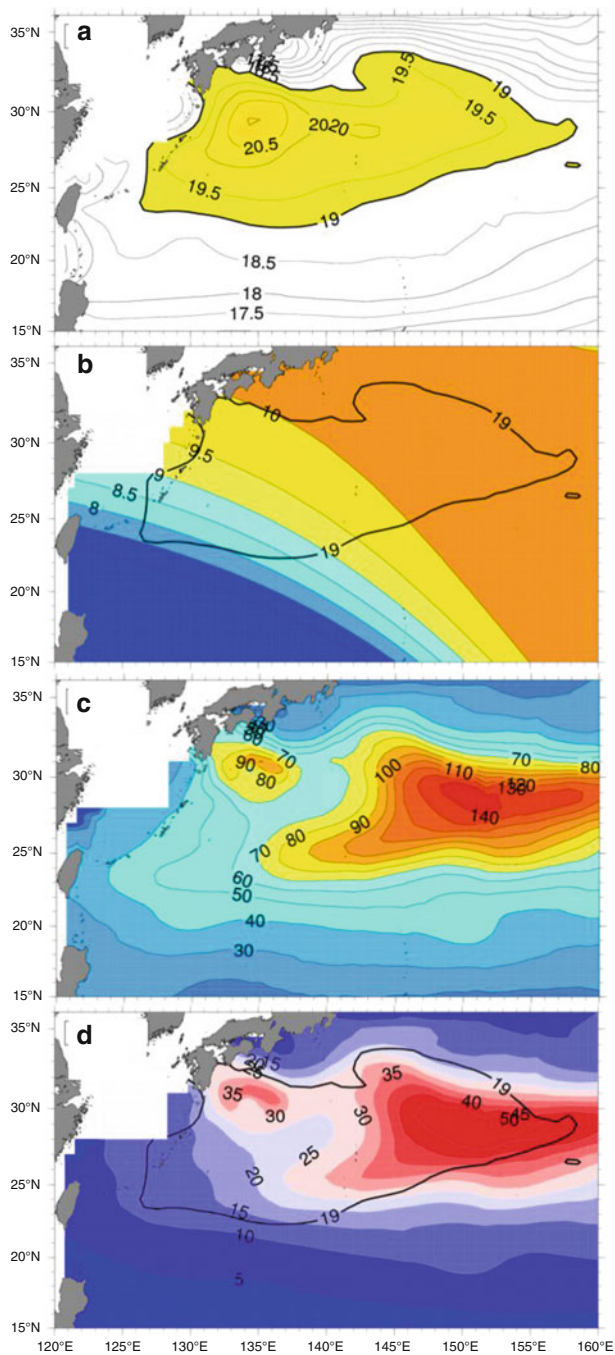


**Fig. 2.9** (a) Acceleration potential on isopycnal surface  $25.3 \sigma_\theta$  referred to 1,000 dbar based on the quality-checked Argo data (resolutions: horizontal  $1^\circ \times 1^\circ$ , vertical 25 layers from surface to 2,000-m depth) during September 2012, which were obtained from [http://www.jamstec.go.jp/ARGO/argo\\_web/argo/index.html](http://www.jamstec.go.jp/ARGO/argo_web/argo/index.html). The area with acceleration potential  $>19 \text{ m}^2 \text{ s}^{-2}$  is colored in yellow.

## 2.5 $^{134}\text{Cs}$ and $^{137}\text{Cs}$ Around Japan Islands

The seawater samples for measurement of  $^{134}\text{Cs}$  and  $^{137}\text{Cs}$  were collected between May 2011, 2 months after the FNPP accident, and March 2014 (Fig. 2.1). In the Japan Sea, the East China Sea, the Seto Inland Sea, and the Bering Sea, only  $^{137}\text{Cs}$  was detected at background levels ( $<2.0 \text{ Bq m}^{-3}$ ), without any detectable  $^{134}\text{Cs}$  (Fig. 2.10). Inoue et al. (2012), Wu et al. (2012), and Kim et al. (2012) reported  $^{134}\text{Cs}$  at trace levels in the Japan Sea, the East China Sea, and around the Korean

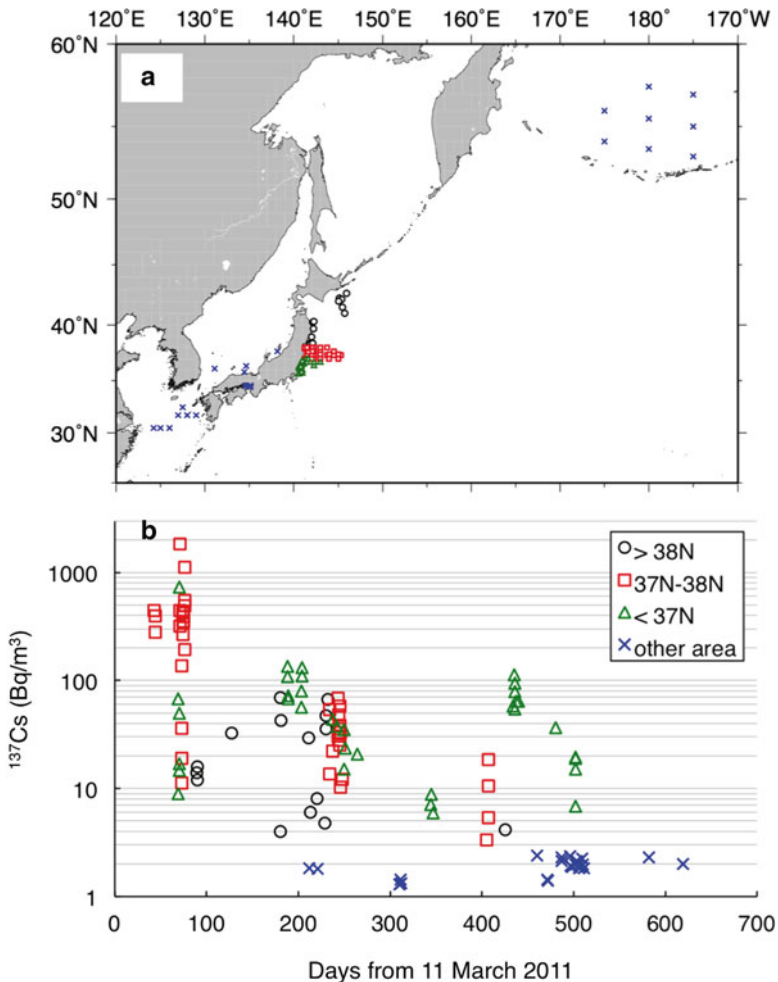


**Fig. 2.10** Sampling locations of surface seawater (a), and temporal variations of  $^{137}\text{Cs}$  in the western North Pacific (b), in the area north of 38°N (open circles), 37°N–38°N (open squares), south of 37°N (open triangles), and in other areas, including the Japan Sea, the Seto Inland Sea, the East China Sea, and the Bering Sea (cross) (Modified from Kaeriyama et al. 2014b)

Peninsula, respectively. These results demonstrated that FNPP-derived radioactive Cs slightly affected the Japan Sea, the East China Sea, the Seto Inland Sea, and the Bering Sea.

In contrast, a high level of radioactive Cs was observed off the coast of East Japan in the western North Pacific (Fig. 2.10). In May 2011, a high concentration of  $^{137}\text{Cs}$ , in excess of  $200\text{ Bq m}^{-3}$ , was observed in the area  $36^{\circ}20'\text{N}$ – $38^{\circ}\text{N}$ , but concentrations were lower than  $100\text{ Bq m}^{-3}$  south of  $36^{\circ}20'\text{N}$  (Fig. 2.11). In the area south of  $36^{\circ}20'\text{N}$ , more than  $500\text{ Bq m}^{-3}$   $^{137}\text{Cs}$  was observed in June 2011, 1 month after our observation (Buesseler et al. 2012). Aoyama et al. (2012) reported temporal variation of radioactive Cs at Hasaki ( $35^{\circ}50.4'\text{N}$ – $140^{\circ}45.6'\text{E}$ ), 180 km south of the FNPP site, during April and December 2011. The peak of radioactive Cs at Hasaki observed in June 2011 represented a delay of 2 months from the appearance of the peak of radioactive Cs at the FNPP site in April 2011. The meso-scale eddy existed in mid-latitudes between FNPP and Hasaki, and its center is located at  $36^{\circ}30'\text{N}$ – $141^{\circ}24'\text{E}$ . This eddy may have prevented the southward transport of FNPP-derived radioactive Cs to Hasaki until the end of May 2011 (Aoyama et al. 2012). The difference in the horizontal distribution of  $^{137}\text{Cs}$  between May and June 2011 (Fig. 2.11) also clearly indicates that the warm core eddy inhibited the southward dispersion of FNPP-derived radioactive Cs along the east Japan coast until the end of May 2011. North of the FNPP, the meso-scale eddy also affected the local

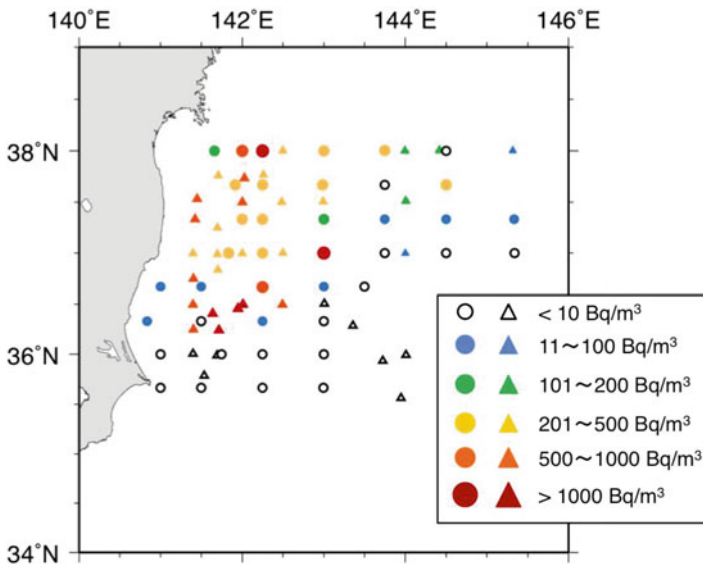


**Fig. 2.11** Sampling locations of surface seawater and  $^{137}\text{Cs}$  concentration in May (circles) and June (triangles) 2011. The data for June 2011 were obtained from Buesseler et al. (2012). Colors of the closed and open symbols indicate the concentrations of  $^{137}\text{Cs}$  (Modified from Kaeriyama et al. 2014b)

distribution of FNPP-derived Cs (Kofuji and Inoue 2013). The patchy distribution of radioactive Cs was also observed around the meso-scale eddy just north of the KE (as shown in Sect. 2.3). To comprehensively understand the patchy distribution of radioactive Cs released from the FNPP, meso-scale-resolved models should be developed.

Figure 2.12 shows temporal variations of  $^{137}\text{Cs}$  off the coast of East Japan based on selected data sets (Aoyama et al. 2012; Buesseler et al. 2011; Kaeriyama et al. 2014b, d; Kaeriyama, unpublished data). To compare the decreasing trend of FNPP-derived radioactive Cs within these data sets, the data of Aoyama et al. (2012) and Buesseler et al. (2011) were plotted from the timing of the observed peak concentration. Exponential decrease was observed in each data set. During the first year from the FNPP accident, drastic decreases of  $^{137}\text{Cs}$  were observed off the east coast of Japan. On the other hand, after 1 year from the FNPP accident, the decay rate seemed to be slower than that of the first year (Fig. 2.12), which may imply that the extremely high radioactive Cs released during March and April 2011 was quickly dispersed from the coastal area to the open ocean within 1 year from the FNPP accident in this area. The weakened decreasing trend apparent after 1 year from the FNPP accident would be affected by new inputs of FNPP-derived radioactive Cs, such as continuing release from the FNPP site, even though continued release was more than four orders of magnitude less than the direct discharge that occurred during March and April 2011 (Kanda 2013). Furthermore, river-borne waters and sediments should have been considered as a long-term source of FNPP-derived radioactive Cs to the ocean. The concentration of  $^{137}\text{Cs}$  obtained from very near coast (off the coast of Onahama; Fig. 2.12) were higher than that of offshore stations (off the east Japan coast and Sendai Bay; Fig. 2.12), possibly caused by the fluvial input of terrestrial FNPP-derived radioactive Cs. Nagao et al. (2013) reported the transport of FNPP-derived radioactive Cs from a contaminated watershed in Fukushima Prefecture to the coastal ocean area during July and December 2011; they estimated the export flux of  $^{134}\text{Cs}$  and  $^{137}\text{Cs}$  after the heavy rain event (Typhoon Roke in September 2011) as roughly  $0.74\text{--}2.6 \times 10^{10} \text{ Bq day}^{-1}$  for the rivers of Fukushima Prefecture. These values account for 30–50 % of the export of radioactive Cs for the 10 months of March 11–December 31, 2011 in these rivers (Nagao et al. 2013). In the future, secondary dispersion of FNPP-derived radioactive Cs through rivers, as considered in Nagao et al. (2013), and through groundwater should be studied to understand the long-term effects of the FNPP accident in the coastal area of East Japan.

---

**Fig. 2.12** (continued) (Kaeriyama et al. 2014b), near the coast of Onahama (*open triangles*) (Kaeriyama, unpublished data), near the coast of Hasaki (*purple open diamonds*) (Aoyama et al. 2012), and near the coast of Iwasawa (*blue open diamonds*) (Buesseler et al. 2011)

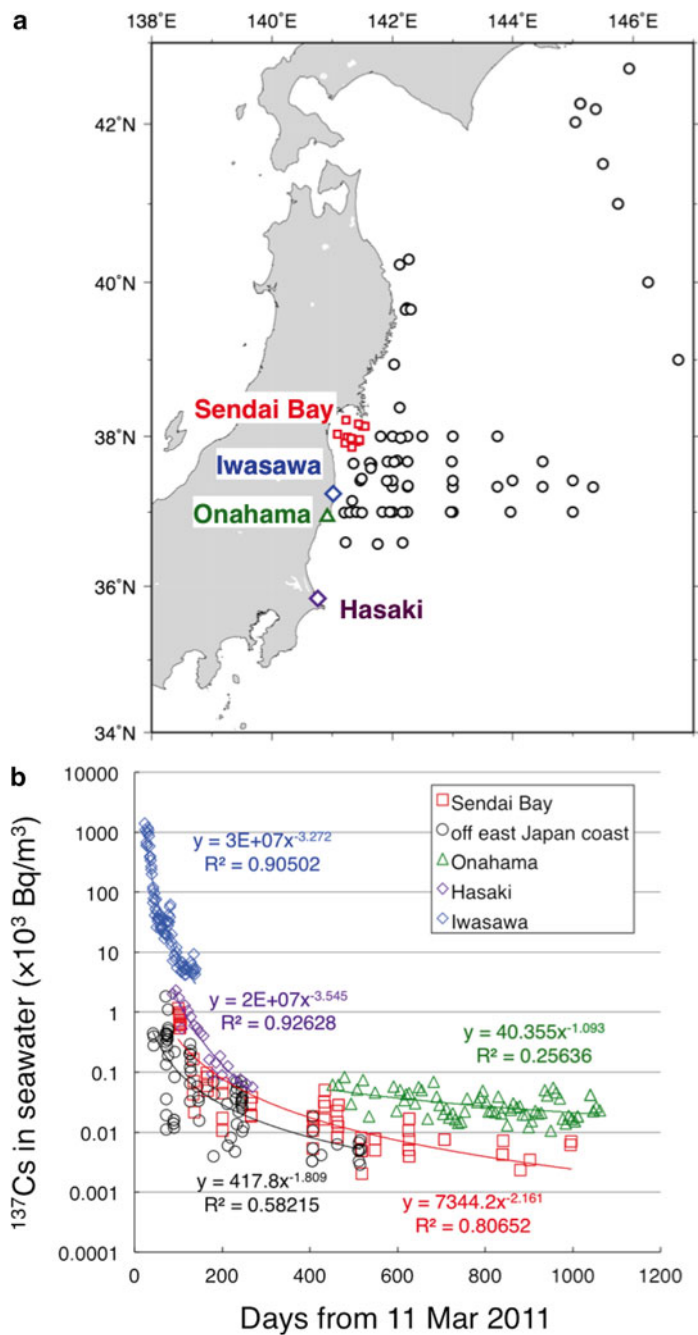


**Fig. 2.12** Sampling locations of surface seawater (a) and temporal variations of  $^{137}\text{Cs}$  (b) in Sendai Bay (open squares) (Kaeriyama et al. 2014d), off the coast of east Japan (open circles)

**Open Access** This chapter is distributed under the terms of the Creative Commons Attribution Noncommercial License, which permits any noncommercial use, distribution, and reproduction in any medium, provided the original author(s) and source are credited.

## References

- Aoyama M, Hirose K, Nemoto K, Takatsuki Y, Tsumune D (2008) Water masses labeled with global fallout  $^{137}\text{Cs}$  formed by subduction in the North Pacific. *Geophys Res Lett* 35. doi:10.1029/2007GL031964
- Aoyama M, Tsumune D, Uematsu M, Kondo F, Hamajima Y (2012) Temporal variation of  $^{134}\text{Cs}$  and  $^{137}\text{Cs}$  activities in surface water at stations along the coastline near the Fukushima Dai-ichi Nuclear Power Plant accident site. *Geochem J* 46:321–325
- Aoyama M, Tsumune D, Hamajima Y (2013a) Distribution of  $^{137}\text{Cs}$  and  $^{134}\text{Cs}$  in the North Pacific Ocean: impacts of the TEPCO Fukushima-Daiichi NPP accident. *J Radioanal Nucl Chem* 296:535–539
- Aoyama M, Uematsu M, Tsumune D, Hamajima Y (2013b) Surface pathway of radioactive plume of TEPCO Fukushima NPP1 released  $^{134}\text{Cs}$  and  $^{137}\text{Cs}$ . *Biogeosciences* 10:3067–3078
- Bailly du Bois P, Laguionie P, Boust D, Korsakissok I, Didier D, Fiévet B (2012) Estimation of marine source-term following Fukushima Dai-ichi accident. *J Environ Radioact* 114:2–9
- Buesseler KO, Aoyama M, Fukasawa M (2011) Impacts of the Fukushima nuclear power plants on marine radioactivity. *Environ Sci Technol* 45:9931–9935
- Buesseler KO, Jayne SR, Fisher NS, Rypina II, Baumann H, Baumann Z, Breier CF, Douglass EM, George J, Madonald AM, Miyamoto H, Nishikawa J, Pike SM, Yoshida S (2012) Fukushima-derived radionuclides in the ocean and biota off Japan. *Proc Natl Acad Sci U S A* 109:5984–5988
- Chino M, Nakayama H, Nagai H, Terada H, Katata G, Yamazawa H (2011) Preliminary estimation of release amount of  $^{131}\text{I}$  and  $^{137}\text{Cs}$  accidentally discharged from the Fukusima Daiichi nuclear power plant into the atmosphere. *J Nucl Sci Technol* 48:1129–1134
- Dietze H, Kriest I (2012)  $^{137}\text{Cs}$  off Fukushima Dai-ichi, Japan: model-based estimates of dilution and fate. *Ocean Sci* 8:319–332
- Ebbesmeyer CC, Lindstrom EJ (1986) Structure and origin of 18°C water observed during the POLYMODE local dynamics experiment. *J Phys Oceanogr* 16:443–453
- Fisheries Agency (2014) Results of the monitoring on radioactivity level in fisheries products. <http://www.jfa.maff.go.jp/e/inspection/index.html> (referred at 20 October 2014)
- Hirose K, Aoyama M (2003) Present background levels of surface  $^{137}\text{Cs}$  and  $^{239,240}\text{Pu}$  concentrations in the Pacific. *J Environ Radioact* 69:53–60
- Honda MC, Aono T, Aoyama M, Hamajima Y, Kawakami H, Kitamura M, Masumoto Y, Miyazawa Y, Takigawa M, Saino T (2012) Dispersion of artificial caesium-134 and -137 in the western North Pacific one month after the Fukushima accident. *Geochem J* 46:e1–e9
- Inoue M, Kofuji H, Nagao S, Yamamoto M, Hamajima Y, Yoshida K, Fujimoto K, Takada T, Isoda Y (2012) Lateral variation of  $^{134}\text{Cs}$  and  $^{137}\text{Cs}$  concentrations in surface seawater in and around the Japan Sea after the Fukushima Dai-ichi Nuclear Power Plant accident. *J Environ Radioact* 109:45–51
- Isoguchi O, Kawamura H, Oka E (2006) Quasi-stationary jets transporting surface warm waters across the transition zone between the subtropical and the subarctic gyres in the North Pacific. *J Geophys Res* 111, C10003. doi:10.1029/2005JC003402
- Itoh S, Yasuda I (2010a) Water mass structure of warm and cold anticyclonic eddies in the western boundary region of the subarctic North Pacific. *J Phys Oceanogr* 40:2624–2642
- Itoh S, Yasuda I (2010b) Characteristics of mesoscale eddies in the Kuroshio-Oyashio extension region detected from the distribution of the sea surface height anomaly. *J Phys Oceanogr* 40:1018–1034



- Kaeriyama H, Ambe D, Shimizu Y, Fujimoto K, Ono T, Yonezaki S, Kato Y, Matsunaga H, Minami H, Nakatsuka S, Watanabe T (2013) Direct observation of  $^{134}\text{Cs}$  and  $^{137}\text{Cs}$  in surface seawater in the western and central North Pacific after the Fukushima Dai-ichi nuclear power plant accident. *Biogeosciences* 10:4287–4295
- Kaeriyama H, Shimizu Y, Ambe D, Masujima M, Shigenobu Y, Fujimoto K, Ono T, Nishiuchi K, Taneda T, Kurogi H, Setou T, Sugisaki H, Ichikawa T, Hidaka K, Hiroe Y, Kusaka A, Kodama T, Kuriyama M, Morita H, Nakata K, Morinaga K, Morita T, Watanabe T (2014a) Southwest intrusion of  $^{134}\text{Cs}$  and  $^{137}\text{Cs}$  derived from the Fukushima Dai-ichi nuclear power plant accident in the western North Pacific. *Environ Sci Technol* 48:3120–3127
- Kaeriyama H, Ambe D, Shigenobu Y, Fujimoto K, Ono T, Nakata K, Morita T, Watanabe T (2014b)  $^{134}\text{Cs}$  and  $^{137}\text{Cs}$  in seawater around Japan after the Fukushima Daiichi nuclear power plant accident. *Oceanogr Jpn* 23:127–146 (in Japanese with English abstract)
- Kaeriyama H, Ambe D, Shigenobu Y, Fujimoto K, Ono T, Watanabe T, Morita T (2014c) Oceanic dispersion of radioactive cesium in the western North Pacific: eastward dispersion in surface water and southward intrusion with mode water. In: Extended abstract of Third International Conference on Radioecology and Environment Radioactivity, OP089, Barcelona, Spain, September 2014.
- Kaeriyama H, Fujimoto K, Ambe D, Shigenobu Y, Ono T, Tadokoro K, Okazaki Y, Takehi S, Ito S, Narimatsu Y, Nakata K, Morita T, Watanabe T (2014d) Fukushima-derived radionuclides  $^{134}\text{Cs}$  and  $^{137}\text{Cs}$  in zooplankton and seawater samples collected off the Joban-Sanriku coast, in Sendai Bay, and in the Oyashio region. *Fish Sci.* doi:10.1007/s12562-014-0827-6
- Kanda J (2013) Continuing  $^{137}\text{Cs}$  release to the sea from the Fukushima Dai-ichi Nuclear Power Plant through 2012. *Biogeosciences* 10:6107–6113
- Kawamura H, Kobayashi T, Furuno A, In T, Ishikawa Y, Nakayama T, Shima S, Awaji T (2011) Preliminary numerical experiments on oceanic dispersion of  $^{131}\text{I}$  and  $^{137}\text{Cs}$  discharged into the ocean because of the Fukushima Daiichi Nuclear Power Plant disaster. *J Nucl Sci Technol* 45:1349–1356
- Kim CK, Byun JI, Chae JS, Choi HY, Choi SW, Kim DJ, Kim YJ, Lee DM, Park WJ, Yim AJ, Yun JY (2012) Radiological impact in Korea following the Fukushima nuclear accident. *J Environ Radioact* 111:70–82
- Kobayashi T, Nagai H, Chino M, Kawamura H (2013) Source term estimation of atmospheric release due to the Fukushima Dai-ichi Nuclear Power Plant accident by atmospheric and oceanic dispersion simulations. *J Nucl Sci Technol* 50:255–264
- Kofuji H, Inoue M (2013) Temporal variations in  $^{134}\text{Cs}$  and  $^{137}\text{Cs}$  concentrations in seawater along the Shimokita Peninsula and the northern Sanriku coast in northeastern Japan, one year after the Fukushima Dai-ichi Nuclear Power Plant accident. *J Environ Radioact* 124:239–245
- Kumamoto Y, Murata A, Kawano T, Aoyama M (2013) Fukushima-derived radiocesium in the northwestern Pacific Ocean in February 2012. *Appl Radiat Isot* 81:335–339
- Kumamoto Y, Aoyama M, Hamajima Y, Aono T, Kouketsu S, Murata A, Kawano T (2014) Southward spreading of the Fukushima-derived radiocesium across the Kuroshio extension in the North Pacific. *Sci Rep* 4:4276–4285
- Masumoto Y, Miyazawa Y, Tsumune D, Tsubono T, Kobayashi T, Kawamura H, Estournel C, Marsaleix P, Lanerolle L, Mehra A, Garraffo ZD (2012) Oceanic dispersion simulations of  $^{137}\text{Cs}$  released from the Fukushima Daiichi nuclear power plant. *Elements* 8:207–212
- Miyazawa Y, Masumoto Y, Varlamov SM, Miyama T (2012) Transport simulation of the radionuclide from the shelf to open ocean around Fukushima. *Cont Shelf Res* 50-51:16–29
- Mizuno K, White WB (1983) Annual and interannual variability in the Kuroshio current system. *J Phys Oceanogr* 13:1847–1867
- Nagao S, Kanamori M, Ochiai S, Tomihara S, Fukushi K, Yamamoto M (2013) Export of  $^{134}\text{Cs}$  and  $^{137}\text{Cs}$  in the Fukushima river systems at heavy rains by Typhoon Roke in September 2011. *Biogeosciences* 10:6215–6223
- Nakano M, Povinec PP (2012) Long-term simulations of the  $^{137}\text{Cs}$  dispersion from the Fukushima accident in the world ocean. *J Environ Radioact* 111:109–115

- Nuclear Regulation Authority (2014) Monitoring information of environmental radioactivity level. <http://radioactivity.nsr.go.jp/en/> (referred at 20 October 2014)
- Oikawa S, Takata H, Watabe T, Misono J, Kusakabe M (2013) Distribution of the Fukushima-derived radionuclides in seawater in the Pacific coast of Miyagi, Fukushima, and Ibaraki Prefectures, Japan. *Biogeosciences* 10:5031–5047
- Oka E (2009) Seasonal and interannual variation of North Pacific Subtropical Mode Water in 2003–2006. *J Oceanogr* 65:151–164
- Oka E, Talley LD, Suga T (2007) Temporal variability of winter mixed layer in the mid- to high-latitude North Pacific. *J Oceanogr* 63:293–307
- Povinec PP, Hirose K, Honda T, Ito T, Scott EM, Togawa O (2004) Spatial distribution of  $^3\text{H}$ ,  $^{90}\text{Sr}$ ,  $^{137}\text{Cs}$  and  $^{239,240}\text{Pu}$  in surface waters of the Pacific and Indian Oceans: GLOMARD database. *J Environ Radioact* 76:113–137
- Qiu B, Chen S (2011) Effect of decadal Kuroshio Extension Jet and eddy variability on the modification of North Pacific Intermediate Water. *J Phys Oceanogr* 41:503–515
- Rypina II, Jayne SR, Yoshida S, Macdonald AM, Douglass E, Buesseler KO (2013) Short-term dispersal of Fukushima-derived radionuclides off Japan: modelling efforts and model–data intercomparison. *Biogeosciences* 10:4973–4990
- Suga T, Hanawa K (1995) Subtropical Mode Water south of Honshu, Japan in the spring of 1988 and 1989. *J Oceanogr* 51:1–19
- Suga T, Aoki Y, Saito H, Hanawa K (2008) Ventilation of the North Pacific subtropical pycnocline and mode water formation. *Prog Oceanogr* 77:285–297
- Sugisaki H, Nonaka M, Ishizaki S, Hidaka K, Kameda T, Hirota Y, Oozeki Y, Kubota H, Takasuka A (2010) Status and trends of the Kuroshio region. In: McKinnel SM et al (eds) PICES special publication 4. Marine ecosystem of the North Pacific Ocean, 2003–2008. North Pacific Marine Science Organization, Sydney, B.C, pp 330–359
- Tsumune D, Tsubono T, Aoyama M, Hirose K (2012) Distribution of oceanic  $^{137}\text{Cs}$  from the Fukushima Dai-ichi Nuclear Power Plant simulated numerically by a regional ocean model. *J Environ Radioact* 111:100–108
- Wu JW, Zhou KB, Dai MH (2012) Impacts of the Fukushima nuclear accident on the China Seas: evaluation based on anthropogenic radionuclide  $^{137}\text{Cs}$ . *Chin Sci Bull.* doi:[10.1007/s11434-012-5426-2](https://doi.org/10.1007/s11434-012-5426-2)
- Yasuda I (2003) Hydrographic structure and variability in the Kuroshio–Oyashio transition area. *J Oceanogr* 59:389–402
- Yasuda I, Okuda K, Hirai M (1992) Evolution of a Kuroshio warm-core ring variability of the hydrographic structure. *Deep-Sea Res* 39(suppl 1):S131–S161